# PRELIMINARY DESIGN AND PERSPECTIVES OF THE EARTHNEXT CUBESAT MISSION FOR EARTH OBSERVATION FROM VERY LOW EARTH ORBIT

**G. Leccese [(1)], S. Natalucci [(1)], L. Iannascoli [(2)], M. Melozzi [(2)], A. Turella [(2)], E. Piersanti [(2)], M. Duzzi [(3)], F. Trezzolani [(3)], G. M. Capuano [(4)], T. A. La Marca [(5)], M. D. Graziano [(6)], M. Grassi [(6)], V. Fortunato [(7)], P. De Marchi [(8)], C. Cardenio [(8)]**

*[(1)] Agenzia Spaziale Italiana, Via del Politecnico snc, 00133 Rome, Italy*
*giuseppe.leccese@asi.it, silvia.natalucci@asi.it*
*[(2)] Officina Stellare, Via della Tecnica 87/89, 36030 Sarcedo, Italy*
*lorenzo.iannascoli@officinastellare.com, mauro.melozzi@officinastellare.com, andrea.turella@officinastellare.com, emanuele.piersanti@officinastellare.com*
*[(3)] T4I - Technology for Propulsion and Innovation, Via Emilia 15, 35043 Monselice, Italy*
*m.duzzi@t4innovation.com, f.trezzolani@t4innovation.com*
*[(4)] TSD-Space, Strada Provinciale per Pianura 2, 80078 Pozzuoli, Italy*
*gmcapuano@tsd-space.it*
*[(5)] Scuola Superiore Meridionale, Largo San Marcellino 10, 80138, Napoli, Italy*
*tobiaarmando.lamarca-ssm@unina.it*
*[(6)] University of Naples "Federico II", Piazzale Tecchio 80, 80125 Naples, Italy*
*mariadaniela.graziano@unina.it, michele.grassi@unina.it*
*[(7)] Planetek Italia, Via Massaua 12, 70132 Bari, Italy*
*fortunato@planetek.it*
*[(8)] AIKO Space, Via dei Mille 22, 10123 Torino, Italy*
*pietro.demarchi@aikospace.com, christian.cardenio@aikospace.com,*

## ABSTRACT

EarthNext is a 16U CubeSat mission, in the framework of ASI ALCOR program, developed by Officina Stellare as prime contractor, that aims at the in-orbit demonstration of VLEO operations for multispectral imaging of the Earth, for land and marine applications. EarthNext preliminary design, with focus on development and testing activities of breadboards for critical/enabling technologies is presented, together with perspectives for the upcoming critical design, verification, launch and commissioning phases.

## 1 INTRODUCTION

Italian Space Agency initiatives dedicated to nano-satellite missions and technologies are collected under the program ALCOR, named as the star of the constellation Ursa Major, that, together with Mizar, forms one of the most famous visual binary systems of the sky. ALCOR symbolizes not only the ability of co-operation with larger space systems, but also the ability to look far away, thus, to innovate. The idea behind the ALCOR program is to create an incubator to ease companies' business, financing prototypes of platforms for innovative services that can then be marketed by developers to place Italy in a condition of consolidated leadership in the sector.
ALCOR missions have been selected throughout the issue of a call for tenders named "Future CubeSat missions" aimed at funding highly innovative nano-satellite projects. The tender resulted in a wide success, with a strong participation of the national CubeSat community. Almost one hundred among companies, mainly Small and Medium Enterprises (SMEs), universities and research centres participated to the call, in most of the cases aggregated in business groups. This participation resulted

in a total of forty-nine proposals presented, twenty of which were selected based on feasibility, innovation and compliance to the national space strategy [1]. The twenty selected missions cover in-orbit demonstrations in all major application domains of the space sector as shown in Figure 1.
In the framework of the ALCOR program, the EarthNext project, led by Officina Stellare (OS) as prime contractor, aims at exploiting Very Low Earth Orbits (VLEOs) to perform effective multispectral Earth observations with CubeSat technology, thus with inherently reduced costs and development times.

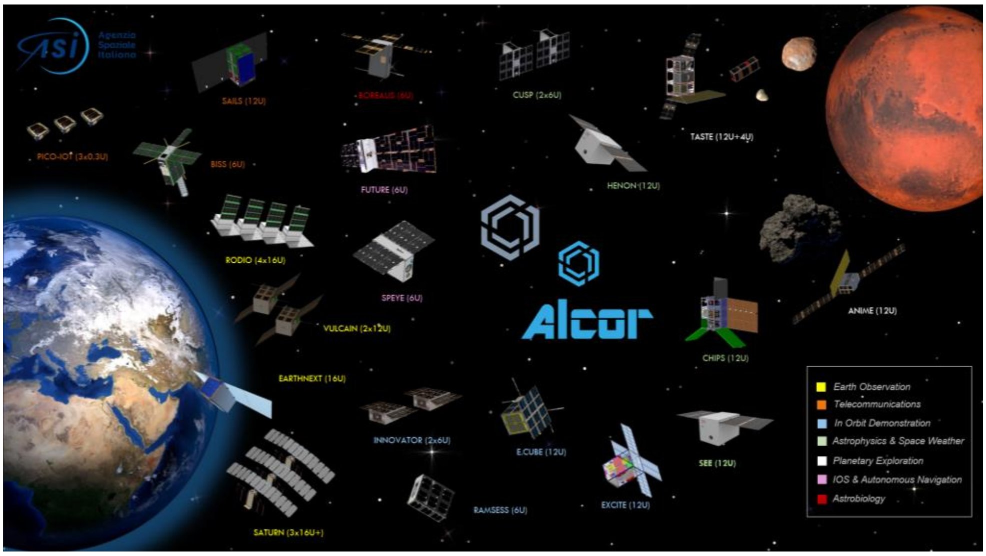

Figure 1. ALCOR program fleet.

VLEOs are very promising for next Earth observation missions due to several advantages they offer, including reduced costs for given performances, due to reduced payload dimensions and launch effort, reduced risks of impacts and need for collision avoidance manoeuvres, with space debris and existing orbiting platforms, as well as an easier disposal at end of life, without dedicated systems and strategies, thanks to a rapid orbital decay. However, associated with mentioned benefits of operating a satellite in VLEO, several critical aspects need to be addressed in the mission and system design. Among these, it must be considered the non-negligible presence of aerodynamic forces, and associated aspects of stability, the reduced communication windows, deriving from the high relative speed to the ground, as well as the erosion from the high presence of atomic oxygen.
EarthNext relies on a 16U CubeSat with 8U allocated for the compact multispectral electro-optical payload and 8U to the platform subsystems. These include several state-of-the-art technologies to address the challenging mission scenario. An integrated electrical propulsion system, using a safe, non-toxic, non-explosive, non-pressurised propellant, is the platform core enabling technology. Beside this, an attitude control system able to perform slow-down manoeuvres to increase time integration over target areas, an electrical power system with deployable solar arrays, a structural system able to withstand atomic oxygen erosion effects, and a state-of-the-art automation capability based on artificial intelligence, to overcome the constraints of conventional operation management, complement EarthNext features.
EarthNext is completing the preliminary design phase, including Bread-Board (B/B) development and testing activities of the three-mirror-anastigmatic telescope, the focal plane array and camera electronics assembly, the on-board computer, the solar panel deployment mechanism and the electrical propulsion system.
In the following, after a general overview of the mission, main outcomes of the preliminary design phase of EarthNext, including breadboard testing lessons learned, together with a roadmap for upcoming detailed design, verification and launch phases, is presented.

## 2 MISSION OVERVIEW

The main objective of the EarthNext mission is twofold. On one hand, EarthNext will demonstrate the viability of operating a CubeSat platform in the VLEO environment through in-orbit demonstration/validation (IOD/IOV) of the capabilities of a compact on-board propulsion system to compensate demanding drag effects and of the spacecraft external surfaces to tackle the severe effects of Atomic Oxygen (AO) impingement. On the other, EarthNext will demonstrate the capability of a CubeSat in VLEO to provide added-value products and services to users in land and marine application fields, through the acquisition of high-resolution multispectral images. Furthermore, a side mission objective will be to augment other reference optical missions by developing and testing data fusion methods with multispectral (e.g. Sentinel-2) or hyperspectral (e.g. PRISMA) data.
Mission targets have been designed to be users-driven, collecting inputs from various potential users and about their pain points. Particularly, the mission-wide Area of Interest (AoI) has been established to cover Italy, as shown in Figure 2. Within the broad AoI a portfolio of pilot case, with several applications purposes, has been selected in order to perform observations for agriculture and aquaculture, city dynamics and forestry [2].


Figure 2. EarthNext mission AoI [3].

Trade-offs performed during phase A study have preliminarily identified the baseline launcher and satellite carrier for the spacecraft injection into the main payload orbit, in a piggy-back launch configuration, at around 500 km and for the transfer into a parking orbit at 400 km, including inclination correction manoeuvres. Once the parking orbit is achieved and commissioning operations of the main sub-systems are completed, the CubeSat will carry out a final transfer into the envisaged target orbit, a sun synchronous VLEO at about 302 km altitude with 10:30 Local Time of Descending Node (LTDN), by means of the on-board propulsion system [2]. The EarthNext mission profile is described in Figure 3.

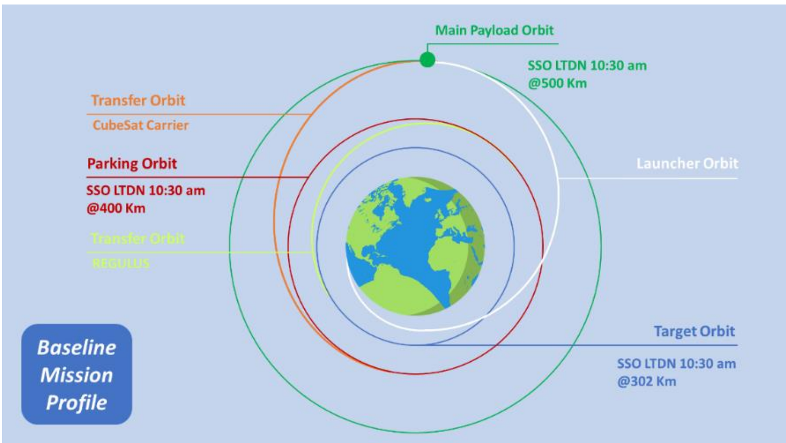


Figure 3. EarthNext mission profile [3].

## 3 SYSTEM PRELIMINARY DESIGN

The EarthNext high level system architecture is depicted in Figure 4.

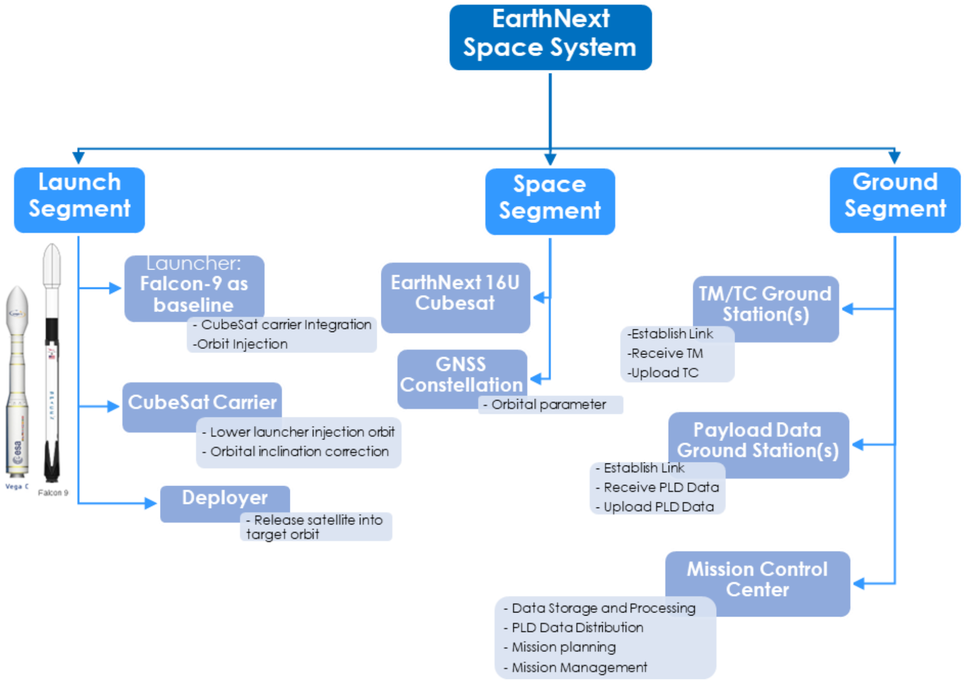


Figure 4. EarthNext system/functional architecture.

### 3.1 Space segment

Focusing on the space segment, EarthNext is designed as a 16Us CubeSat platform, operating at the lower end of the micro-satellite mass range. The satellite bus can be split into the following main subsystems: Payload and Platform Data Subsystem (PPDS), Guidance, Navigation and Control (GNC), Electrical Power Subsystem (EPS), Communications (COM), Propulsion (PRP), PPDS Flight Software (FSW), Structure, Harness and Mechanism (MEC), Thermal Control Subsystem (TCS).
The Global Navigation Satellite System (GNSS) constellations, listed within the space segment block diagram, act as a service to obtain position and velocity information of the spacecraft.

### 3.2 Ground segment

The EarthNext ground segment will consist of a Mission Operations Center (MOC) located in Bari, that comprises**:** a Flight Operations Segment (FOS), a Payload Data Ground Segment (PDGS), a Performance Assessment Segment (PAS), a Ground Stations Network (GSN).
It has been chosen to de-couple the GSN by using commercial services of GSaaS. The baseline has been identified with LeafSpace, facilities for satellite control and monitoring, thus TMTC, and payload data downloading. KSAT and Amazon Web Services (AWS) are also considered as backup solution, to be integrated where needed. The feasibility of employing ASI facilities in the LEOP phase has to be verified.

### 3.3 Launch segment

In order to place the satellite into the target orbit, as depicted in Figure 3, the EarthNext launch segment will consist of a Falcon 9 or Vega-C launch vehicle, as baseline, combined with a CubeSat Carrier. To perform the transfer manoeuvre to parking orbit at about 400 km, D-Orbit's ION platform has been selected as baseline carrier. The following back-up launchers will also be envisaged: Electron, Vega-E, SSC SmallSat Express.

## 4 BREADBOARD DEVELOPMENT AND TESTING

As part of the EarthNext project phase B, through the Preliminary Design Review (PDR), breadboard development and testing activities have been carried out to advance the enabling technologies, demonstrating the necessary performances and capabilities to de-risk mission phase C/D. Breadboarding activities addressed the following subsystems:

- The Three-Mirror-Anastigmatic (TMA) telescope by OS, to pre-test alignment criticality and alignment capability;
- The Focal Plane Array (FPA) and the camera electronics (CE) assembly by Techno System Developments (TSD), to demonstrate the viability to attach the multispectral optical filters directly on the large area imager (technologically demonstrated on smaller imagers from the same manufacturer) and to downscale the electronics;
- The On-Board Computer (OBC), along with a B/B version of the on-board software, to demonstrate the feasibility of scaling down TSD's standard on-board computers to CubeSat size, while also improving the computational capacity to implement on-board deep learning algorithms;
- The Solar Panel Deployment Mechanism (SPDM) by OS to demonstrate the viability of the solar panel release effectiveness;
- The electrical propulsion system by Technology for Propulsion and Innovation (T4I), to demonstrate the achievement of the necessary performances to operate in the VLEO environment.

### 4.1 Three-mirror anastigmatic telescope

The functional requirements which have driven the telescope optical design are reported in Table 1.

Table 1. Functional Requirements.

| Requirement title | Requirement | Required value |
|---|---|---|
| Spatial sampling | The Ground Sampling Distance (GSD) at nadir shall be in the range 2 - 5 m | 2 - 5 m @ nadir |
| ACT swath | The payload ACross-Track (ACT) swath width shall be larger than 12 km | >12 km |
| Operating altitude | The spacecraft shall operate at an altitude between 290 and 310 km | 302 km |
| Payload envelope | EarthNext electro-optical payload shall fit within an 8U envelope | ≤ 8U |
| Spectral channels | Operative spectral channels shall be in the range 440-900nm. | 440 – 900 nm |

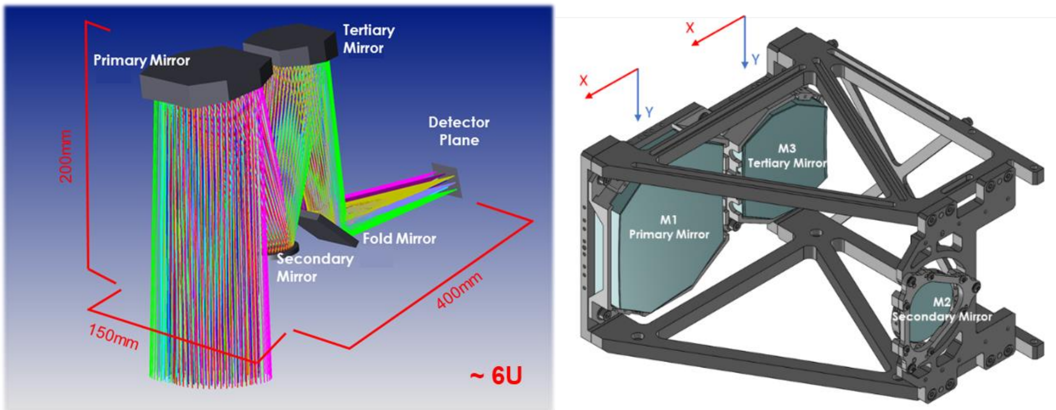


Figure 5. (Left) Optical schematics of EarthNext TMA. (Right) TMA BB optomechanical design.

The TMA configuration proved to be the best architecture for the EarthNext payload to cope with the mission/system requirements, particularly matching the limited envelope available inside the CubeSat platform. The main features of the TMA design illustrated in Figure 5 are reported in Table 2.

Table 2. EarthNext TMA main characteristics.

| **Parameters** | **Design results** |
|---|---|
| Focal length | 500 mm |
| Relative aperture | F/ 6.3 |
| Field of view | 3 x 1.5 deg |
| Distortion | 0.50% |
| Pixel size | 6.4 µm |
| GSD @ nadir | 3.9 m |
| ACT swath width | 17 km |

Although the structure of the B/B telescope has been designed with a similar architecture to that of the expected flight model, there are some differences. Particularly, since the FPA would not be tested on the B/B, the part of the structure designed to accommodate it was not manufactured; furthermore, the folding mirror, shown in Figure 5, was not included in the B/B either, since its only function is to deflect the light path towards the focal plane. These design discrepancies are in any case negligible: the developed TMA B/B catches all the criticalities inherent to the chosen optomechanical configuration.
The goal of the telescope breadboarding has been to align the payload mirrors, that is to make all mirror axes coincident, and to locate the three optical elements at the correct distance among them, to achieve the required optical performance. A secondary objective has been to verify the in-house production capabilities of off-axis aspherical mirrors with demanding optical requirements, as shown in Figure 6.

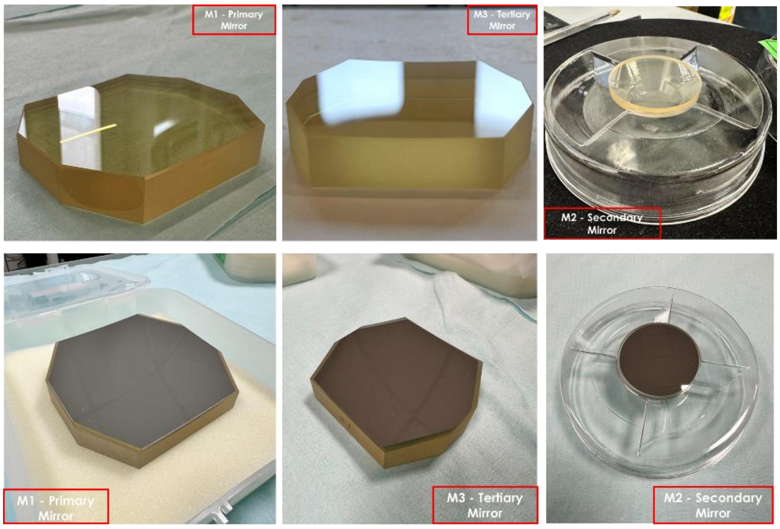


Figure 6. (Top) Primary, tertiary and secondary mirrors of TMA B/B.
(Bottom) Primary, tertiary and secondary mirrors of TMA B/B coated with OS silver coating.

TMA alignment is accomplished when the required Transmitted WaveFront Error (TWFE) is measured with interferometer or other suitable means, e.g. Shack Hartmann test. In further details, the TMA alignment pass/fail criteria can be express as follows: on field, i.e. across a rectangle of

3x1.5 degrees centred on the telescope axis, the TWFE shall be less than 152 nm RMS with double-step measurement. This corresponds to a single-step TWFE on field less than 76 nm RMS.
Figure 7 shows the B/B of the TMA and the test setup that was used for the alignment of its three mirrors and to perform the interferometric measurements. The TMA B/B was placed on an optical table and fixed on a motorized rotary stage and a tiltable support in front of a Zygo DinaFiz interferometer; the optical setup was completed with a spherical return mirror placed on a triaxial stage.

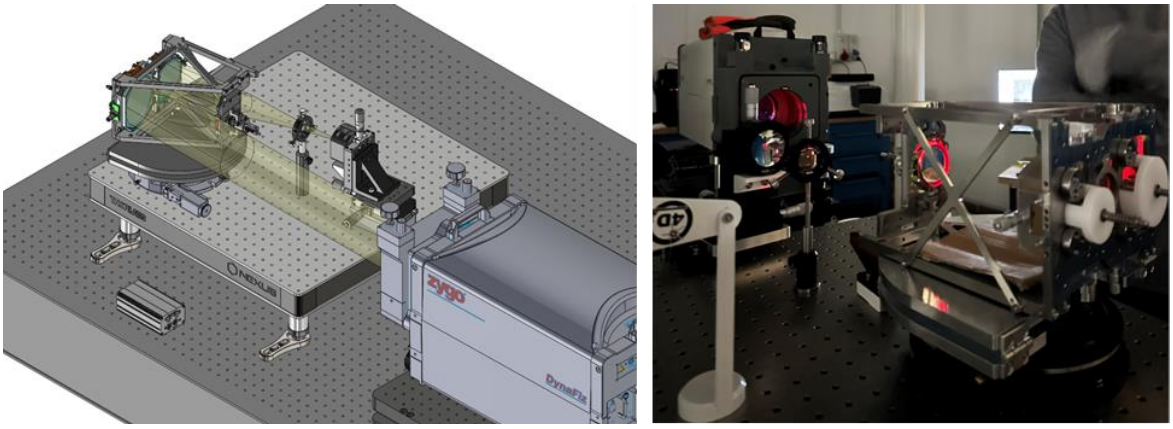


Figure 7. TMA B/B test setup: (Left) CAD representation and (Right) B/B model during TWFE measurement.

When align TMA telescopes, mirror fine mechanical movements should follow established rules to null spherical aberration, coma and astigmatism at the focal position (the foci of the offset field angle). Following mirror integration TMA showed some severe astigmatism and coma, as depicted in Figure 8 (Top).

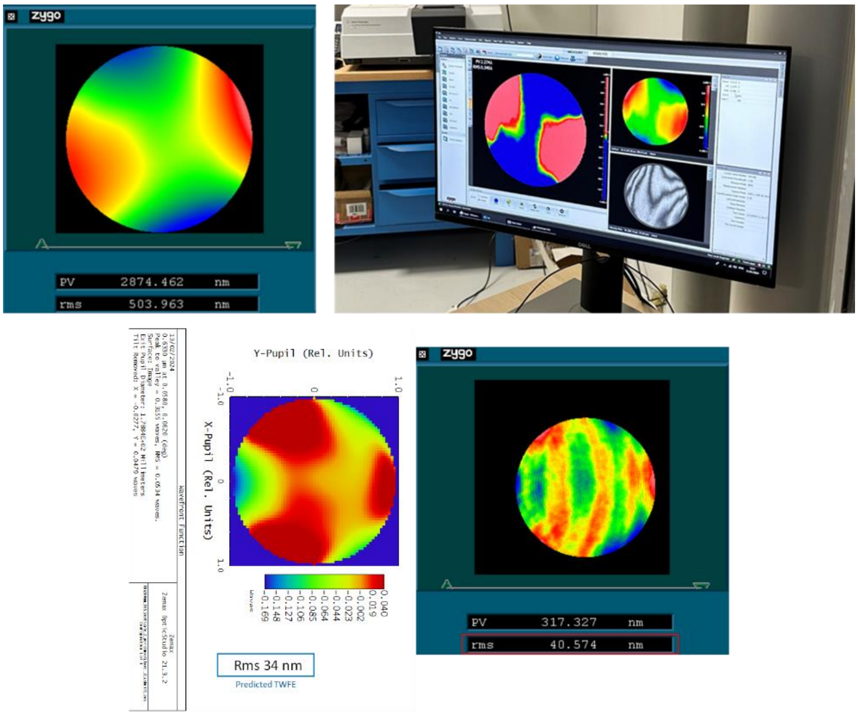


Figure 8. (Top) TWFE following integration: simulated, on the left side, and measured, on the right side, at the beginning of the alignment campaign. (Bottom) On axis measured TWFE, on the right side compared with simulation, on the left side, at the end of the alignment campaign.

TWFE measurements were also performed at some field positions. It has been verified that also at Y field angles ±0.75 deg, the most critical direction for TMA telescopes, as well at X field, measurement results are coherent with simulation indicating that TMA has been correctly aligned. All measurement indicates that double pass TWFE is lower than the stated pass/fail criteria: in the wors case scenario, +0.75 deg in Y direction, measured TWFE is equal to 126 nm < 152nm RMS.

### 4.2 Focal plane array and camera electronics assembly

The multispectral camera is characterized by a very innovative design solution, ensuring a very compact architecture. The camera is composed of two thermo-structurally decoupled assemblies. The FPA, hosting the detector and the proximity electronics, is connected to a separate and stand-alone main CE by means of flexible PCB-based links. The camera features several thermo-structural, electrical and electronics items, aimed at acquiring the images and ensuring a very accurate positioning of the focal plane with respect to the overall telescope assembly.
The CE is based on highly integrated electronics, and it offers a wide set of functionalities such as detector configuration and control/synchronization, image data acquisition, and pre-processing, including pixel equalization to uniformize the detector radiometric response.
The FPA has been designed to accommodate the CMV20000 detector, a COTS CMOS image sensor by CMOSIS with a resolution of 5120x3840 pixels. The multispectral imager implements a spatio-spectral scanning acquisition mode. It is based on the adoption of a filter array that transfers the selected spectral wavelengths of the optical signal to different regions (sub-stripes) of the 2D image sensor. It comprises a set of six spectral bands and will be fixed above the detector array.
The engineering model of the FPA and its I/F and power module, that is part of the CE, have been already developed in the frame of the phase B breadboarding activities. The FPA test results will be presented during the symposium.

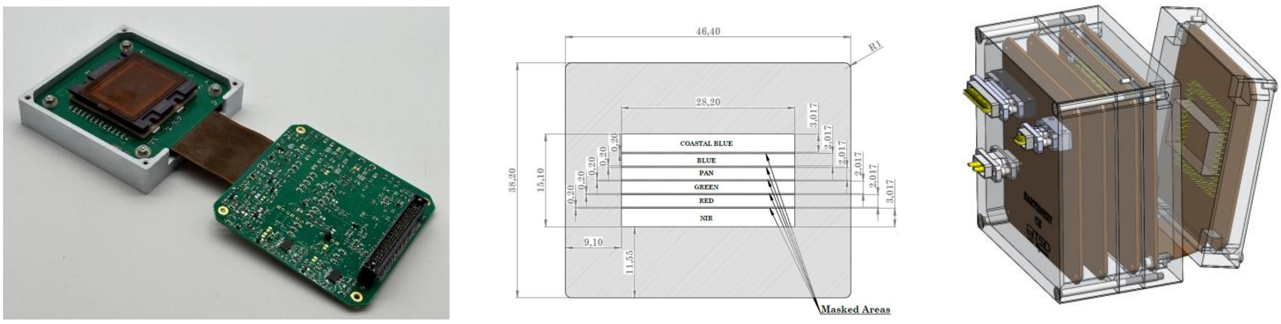

Figure 7. FPA B/B, multispectral filter configuration, FPA and CE CAD.

### 4.3 On-board computer

The avionics architecture is based on an integrated data system, named “Platform & Payload Data System (PPDS)”, able to support both the platform and the payload data handling and processing. Thanks to the very high integration level of the PPDS, it became possible to provide a complete set of functionalities, typically available onboard larger satellite platforms than a 16U CubeSat.
The OBC, whose block diagram is shown in Figure 8, is the main component of the PPDS. The OBC performs the control and management of all the avionics and electro-optical payload subsystems. The OBC is characterized by a distributed hardware and software design, based on two subsystems.
The hardware and software architecture for the Central Data Handling & Processing (CDH&P) is based on Rad-Tolerant PolarFire FPGA to ensure high reliability and robustness in the space radiation environment. The FPGA integrates the RISC-V architecture as soft-core CPU, for the execution of the Application Flight Software, and other VHDL modules for real-time payload data processing such as compression, data handling and storage.

The Processing Hardware Accelerator (PHA) leverages the advanced capabilities of Microchip's PolarFire System on Chip (SoC) that combines a powerful hard multicore RISC-V microprocessor, with the FPGA fabric in a single device. The SoC's hardware and software architecture is designed to enable the deployment of AI-based algorithms onboard spacecraft. The programmable logic is configured to accelerate challenging computational workflows such as those required by deep learning-based inference processes.
The OBC B/B tests are ongoing and will be part of the presentation to be held during the symposium.

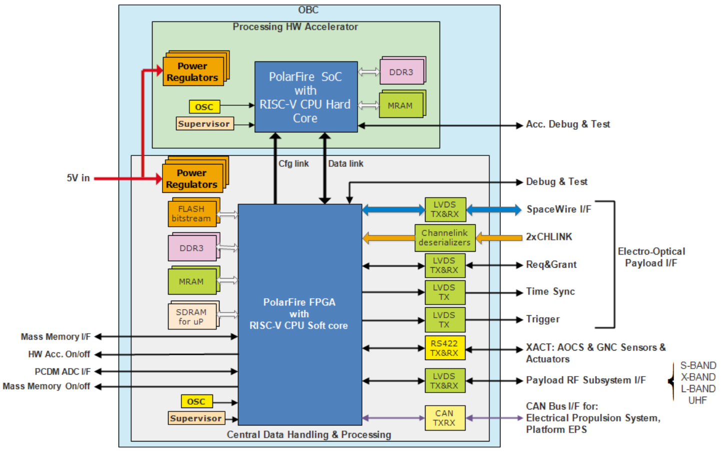


Figure 8. OBC block diagram.

### 4.4 Solar panel deployment mechanism

The SPDM, designed as a B/B for EarthNext, is based on a burn wire approach. This approach consists of retaining the solar panels, in stowed configuration, to the satellite body frame using a polymer wire or rope which will then be thermally cut using a resistor. Burn-wire solutions have an extensive heritage in the CubeSat framework. Since the most common failure mode for burn wire mechanisms is a partial fusion of the wire, two requirements have been set:

- The release mechanism shall include a driving system which has the task of ensuring that the resistor completely passes through the polymer wire;
- The release mechanism shall be fail-safe, i.e. shall include two independently powered initiator as to make it redundant.

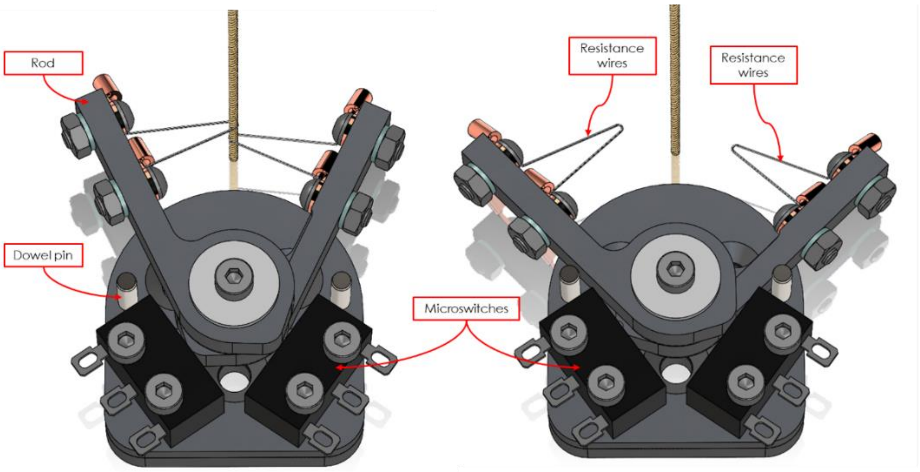


Figure 9. CAD representation of SPDM BB: (Left) in the enabling state (Left) and (Right) in the final state (Right), i.e. after rope cutting.

As depicted in Figure 9, each release mechanism contains two resistors, made of resistance wire, which are independently powered using faston terminals. The driving system consists of a torsion spring which is hosted inside dedicated pockets that were milled in the rods. Two press fit dowel pins, that act as end stops, and two micro-switches, that independently activate when a rod has reached its end stop, have been also added to the design. Micro-switches give information on the state of the mechanism after its activation, thus detecting any non-standard behaviour of the system. The micro-switches allow also to precisely measure the time needed to thermally cut the wire, thus providing a metric to assess the effectiveness of the SPDM. Two resistance wire materials have been employed for the B/B, Nichrome60 and Kanthal A1, as well as two rope material, Vectran rope (Ø0.9 mm) and Dyneema SK75 rope (Ø0.9 mm). Both resistive wire and rope materials have been extensively used in space applications.
The objective of SPDM B/B was to demonstrate the viability of the solar panel release effectiveness, i.e. to demonstrate that burn-wire mechanism was able to fully trim the hold-down rope. A partial trim is not acceptable. A graphical representation of this criteria is given in Figure 10.

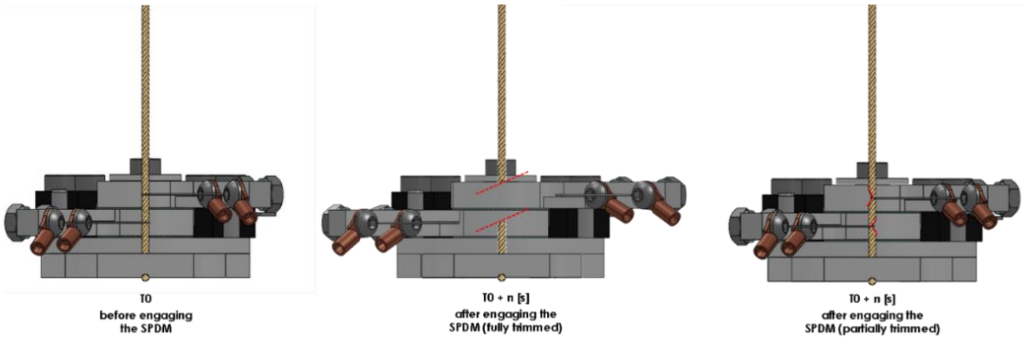


Figure 10. SPDM B/B pass/fail criteria: graphical representation.

First, a rope characterization campaign (tensile testing) has been carried out to estimate the ultimate tensile strength of the Dyneema and Vectran ropes. The tensile tests showed that all ropes have a tensile strength well above the estimated 50-200 N preload required to keep the solar panels stowed during launch. The release mechanism was then tested both in air at 20 °C and in a thermal vacuum chamber, at -30 °C and +70 °C, to evaluate its behaviour in the expected temperature range, acquiring data on the elapsed time to cut the rope and testing different resistor/rope material combinations. A dedicated test setup was designed to accommodate five release mechanism, as shown in Figure 11, providing required preload to the ropes by means of dedicated compression springs. As described in [4], concerning a similar burn-wire mechanism, it was decided to supply the resistors with a nominal current equal to 1.6 A.

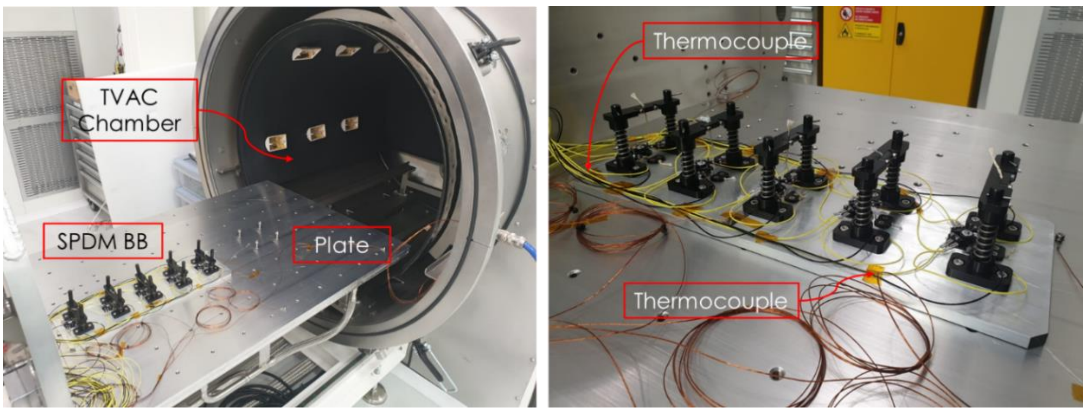


Figure 11. (Left) SPDM test setup inside the TVAC chamber. (Right) BB setup and thermocouples.

The different combinations of resistance wire and rope that have been tested are:

- Kanthal A1/Vectran Ø0.9mm (one mechanism)
- Kanthal A1/Dyneema Ø0.9mm (one mechanism)
- Nichrome60/Vectran Ø0.9mm (two mechanisms)
- Nichrome60/Dyneema Ø0.9mm (one mechanism)

It was decided to collect more data on Vectran rope because it has an extremely low coefficient of thermal expansion and almost no creep, factors that make it particularly suitable for ensuring that an almost constant preload is kept between the solar panels and the satellite body. During the test, the cut-off times were recorded on an oscilloscope by measuring the time elapsed between the start of the current flow in the resistors and the drop in the micro-switches' signals, as shown in Figure 12.

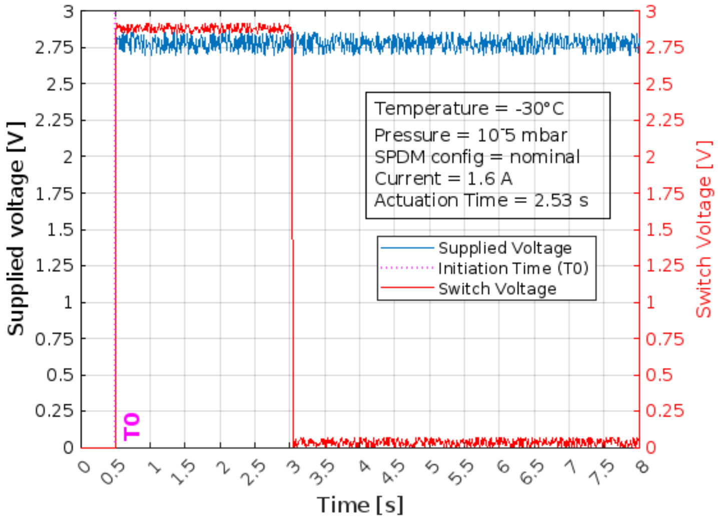


Figure 12. Actuation: signals reading from the oscilloscope during the activation of the mechanism.

The test setup with the five mechanisms was fired five times in vacuum: three times at +20 °C, i.e. each of the five mechanism was fired three times; one time at -30 °C, i.e. each of the five mechanism was fired one time; one time at +70 °C, i.e. each of the five mechanism was fired one time. No failures were detected. The average cut-off times are listed in Table 3.

Table 3. Release test in TVAC: average cut-off times.

| Resistance wire/rope | Average cut-off time |
|---|---|
| Nichrome60/Vectran | 2.94 s |
| Nichrome60/Dyneema | 2.53 s |
| Kanthal A1/Vectran | 3.00 s |
| Kanthal A1/Dyneema | 2.44 s |

Fail-safe, i.e. contingency, configurations have also been tested. The release mechanism was fired five times considering, in the first case, the loss of one resistor and, in the other, a lower supply current than the nominal 1.6 A value. Loss of one resistor have brought to a slight increase in the time required to cut the ropes, without any relevant impact on performance, while even considering lower than nominal values of current, all the mechanisms were able to successfully cut the rope.

### 4.5 Electrical propulsion system

To fulfill the EarthNext mission requirements, an advanced B/B model of the REGULUS-50-I2 electrical propulsion system by T4I (marked as REGULUS-50-I2 L), has been developed and tested.

REGULUS-50-I2 is a complete electric propulsion unit fed with iodine propellant which relies on the Magnetically Enhanced Plasma Truster (MEPT) technology. The main functional requirements which have driven the REGULUS-50-I2 S redesign were:

- Total impulse equal to 11 kNs
- Unregulated input voltage equal to 12 V

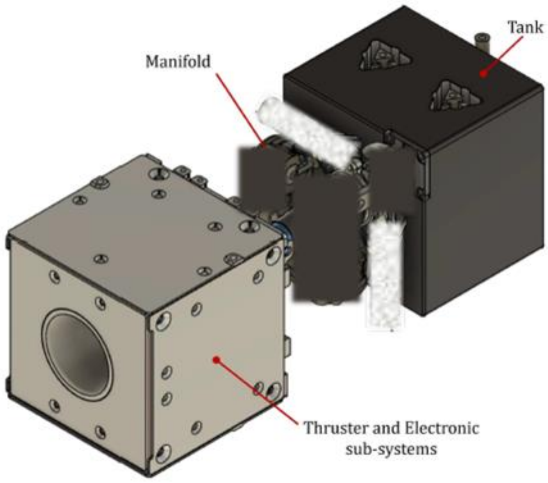


Figure 13. CAD representation of the REGULS-50-I2 L. The electronics to manage the unregulated input voltage is not shown in the figure. In the BB, the injector is longer than the final one to ease the assembly and allow standalone tests of the subsystems.

The system B/B is composed of the following subsystems:

- The thruster head, comprising the MEPT, which provides propulsion;
- The electronics sub-system includes three boards, all located around the MEPT inside the thruster sub-system, and a separate B/B model of the Power Processing Unit (PPU). This board manages the input voltage, and controls valves and heaters;
- The fluidic sub-system, which includes the propellant tank, redesigned to store up to 2.5 kg of iodine propellant to achieve a total impulse of 11 kNs, and the propellant feed system, to provide the defined mass flow rate.

The REGULUS-50-I2 L breadboard has implemented several improvements, including:

- A re-designed fluidics sub-system, with optimized thermal and fluidic line design to reduce/eliminate the transient phase upon propulsion activation;
- An improved thermal control of electronic boards;
- A higher maximum heating power, brought from 20 W to 40 W, to speed up the heating phase if supported by the platform;
- New PPU boards to manage unregulated input voltage.

The PPU-power board is the power interface between REGULUS and the spacecraft and is basically a multi-output DC-DC converter, providing the required voltage and current supply to the various sub-systems of REGULUS. Being essentially a functional demonstrator, the PPU-power board, depicted in Figure 14, has an envelope of approximately 180x100x337 $mm^3$, and it will be optimized and miniaturised of the final design. Several standalone tests were performed on the thruster head, fluidic sub-system, and electronic sub-system of the propulsion B/B, such as: iodine mass flow estimation by means of mass loss measurements, pressurization up to maximum expected operating pressure with N2 gas, conditioning boards verification, power and radiofrequency boards verification, verification of boards behavior in case of load variations (safety systems). Following standalone verification, a test campaign on the fully integrated REGULUS-50-I2 L B/B were carried out. The integrated tests first concerned communication, sensor reading, RF output power and DC-AC efficiency verification as well as valves and heaters actuation. The results obtained from this first campaign were satisfactory and highlighted the bottleneck of B/B model, to be optimized in the next project phase. What emerged was that PPU DC-DC converter produces an efficiency much lower (65%-80%) than expected (90%).

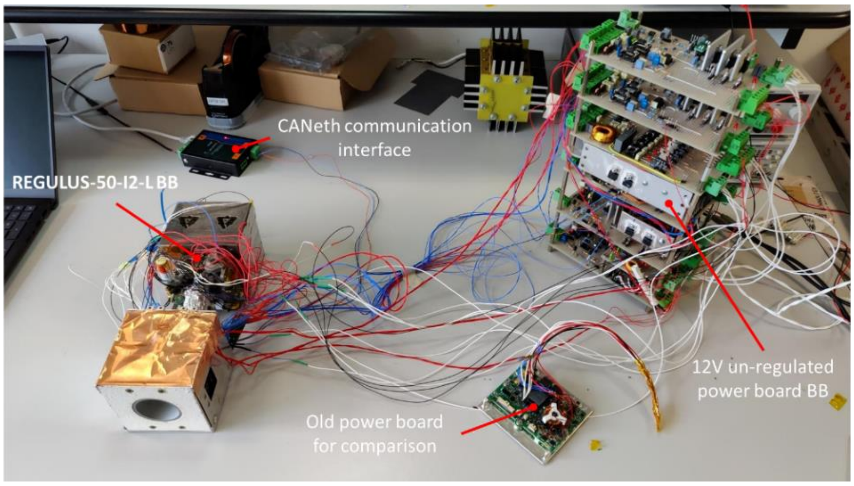


Figure 14. REGULUS-50-I2-L BB with 12V unregulated power board and communication I/F.

Last integrated test consisted in a full-scale performance verification at REGULUS BB system level. The test was carried out in the T4I's vacuum chamber. The facility is provided with a Faraday probe, and a thrust balance as shown in Figure 15. The thrust balance is specifically designed to test RF plasma thrusters and features a counterbalanced pendulum architecture. Thrust is correlated to the movement of the rotating arm of the balance, which is measured with a high-resolution laser interferometer capable of detecting displacements well below 1 micron, against a typical sensitivity on the order of at least 10-15 µm/mN.

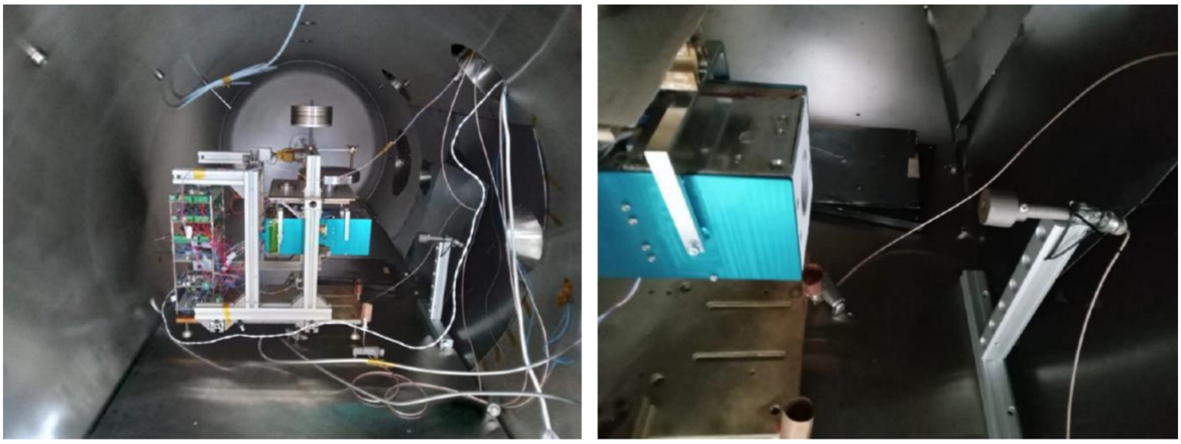

Figure 15. (Left) REGULUS-50-I2-L B/B on T4I's thrust balance. (Right) Detail of the positioning of the Faraday probe. The latter is in axis with the thruster at a distance of 130 mm.

During the tests, REGULUS-I2-L B/B was first brought to high vacuum, vented to remove air from inside the fluidics and then heated up to firing condition (Figure 16). Once ready, thrust was measured for various power levels by igniting plasma, switching it to steady state and then leaving it on for 1-2 minutes before turning it off, to produce a net "jump" on the thrust balance. The new fluidic sub-system provided very good results, producing reliable ignition with very fast transition between ignition and steady-state conditions. Regarding performance thrust to power ratio is on the average equal to 0.3 mN at 55 W thus lower than the target value of 0.5 mN ±10% at same supply power. Although this discrepancy occurred, the reduction is in line with expectations coming from PPU board characterization tests, i.e. once the reduced efficiency of the B/B 48V converter is taken into account. An optimization phase is already foreseen at the beginning of phase C to increase the efficiency of the DC-RF conversion circuit, along with the board miniaturization. Faraday probe measurements provided an interesting indication, in that the output of the probe (which is proportional to the collected ion current) is almost constant as RF power is varied. This indicates that the probe is, in fact, in ion saturation current regime.

Figure 16. REGULUS B/B firing. The bright yellow colour of the plume is typical of iodine plasma.

## 5 PROJECT PERSPECTIVES

The EarthNext mission phase C/D/E1 follow up is now under ASI board approval. The phase C/D/E1 will last 40 months overall, including 28 months of phase C/D and 12 months of phase E1.

During phase C, the qualification status of Components Off The Shelf (COTS) will be assessed through a relevant Equipment Qualification Status Review (EQSR). After that, verification activities at equipment/sub-system level will be conducted and the system detailed design consolidated, targeting the Critical Design Review (CDR).
During phase D, at satellite level, after relevant Test Readiness Reviews (TRRs), verification through testing activities will be carried out according to the following model philosophy:

- A CubeSat Structural and Thermal Model (STM) that will be used for the validation of the structural design. It will be subject to structural testing at qualification levels and durations;
- A CubeSat Engineering Model (EM) that will complement the representativeness of the STM with the equipment/sub-system Engineering Qualification Models (EQMs), thus integrating electrical/data interfaces;
- A CubeSat Proto Flight Model (PFM) that will be the final product after integration, and it is the model that will be launched. It will be subject to a complete proto-flight test campaign, thus qualification levels with acceptance duration.

After the launch, which is foreseen in Q2/Q3 of 2027, a one-year phase E1 will be conducted, including 6 months of transfer to the selected VLEO and 6 months of actual CubeSat commissioning, preparing for the operational routine lifetime.

## 6 CONCLUSIONS

EarthNext is a 16U CubeSat mission, in the framework of ASI ALCOR program, developed by Officina Stellare as prime contractor, that aims at the in-orbit demonstration of VLEO operations for multispectral imaging of the Earth for land and marine applications. EarthNext is concluding the phase B, which has foreseen the preliminary design for both space and ground segment as well as extensive breadboarding activities of critical/enabling technologies. The breadboard of the on-board computer, of the focal plane array and camera electronics assembly have been developed and are ongoing testing activities. The breadboard of the three-mirror anastigmatic telescope, of the solar panel deployment mechanism and of the electrical propulsion system have been on the other hand successfully completed. For the latter, improvement activities of the PPU power conversion efficiency are foreseen at the beginning of phase C in order to fully match the needed thrust level in nominal electrical power conditions. Phase C/D/E1 is under ASI board approval, encompassing 28 months of phase C/D and 12 months of phase E1, including the transfer to the selected VLEO and the system commissioning. The EarthNext launch is currently scheduled for Q2/Q3 2027.

## 7 REFERENCES

[1] Leccese G., Natalucci S., Fedele A. and Cottini V., *Overview and roadmap of Italian Space Agency activities in the micro- and nano-satellite domain*, 73rd International Astronautical Congress (IAC), Paris, France, 2022.

[2] Iannascoli L., Turella A., Piersanti E., Duzzi M., Capuano G., Grassi M., Graziano M. D., Fortunato V., De Marchi P., Leccese G., Rinaldi M., Terracciano A., Di Clemente M., Luciani R. and Natalucci S., *EarthNext: a very low Earth orbit cubesat mission for multispectral Earth observation*, 74th International Astronautical Congress (IAC), Baku, Azerbaijan, 2023.

[3] Leccese G., Natalucci S., Di Clemente M., Luciani R., Rinaldi M., Iannascoli L., Turella A., Piersanti E., Duzzi M., Capuano G., Graziano M. D., Fortunato V. and Madonia P. G., *EarthNext cubesat mission and system study for multispectral Earth observation from very low Earth orbit*, 14th IAA Symposium on Small Satellites for Earth System Observation, Berlin, Germany, 2023.

[4] Thurn, A., Huynh, S., Koss, S., Oppenheimer, P., Butcher, S., Schlater, J., & Hagan, P. (2012, May). A nichrome burn wire release mechanism for CubeSats. In The 41st Aerospace Mechanisms Symposium, Jet Propulsion Laboratory (pp. 479-488).